First Measurement of the Photon Structure Function $F_{2,c}^{\gamma}$

Richard Nisius (OPAL Collaboration)[1]

CERN, CH-1211 Genève, Switzerland, Richard.Nisius@cern.ch

Abstract. The first measurement of $F_{2,c}^{\gamma}$ is presented. At low x the measurement indicates a non-zero hadron-like component to $F_{2,c}^{\gamma}$. At large x the measurement constitutes a test of perturbative QCD at next-to-leading order, with only m_c and α_s as free parameters, with a precision of $\mathcal{O}(40\%)$.

INTRODUCTION

For about 20 years measurements of photon structure functions give deep insight into the rich structure of a fundamental gauge boson, the photon. A recent review on this subject can be found in [1]. Here, the discussion is restricted to the measurement of $F_{2,c}^{\gamma}$, which recently has been achieved for the first time. Only the main features of the analysis are given, the experimental details can be found in [2].

The differential cross-section for deep inelastic electron-photon scattering, shown in Figure 1, is given by

$$\frac{\mathrm{d}^2\sigma}{\mathrm{d}x\,\mathrm{d}Q^2} = \frac{2\pi\alpha^2}{x\,Q^4}\left[\left(1+(1-y)^2\right)F_2^{\gamma}(x,Q^2) - y^2 F_{\mathrm{L}}^{\gamma}(x,Q^2)\right]. \qquad (1)$$

Here Q^2 is the absolute value of the four momentum squared of the exchanged virtual photon, $\gamma^{\star}$, x and y are the usual dimensionless variables of deep inelastic scattering and α is the fine structure constant. In experimental analyses y^2 is usually small. Consequently, the term proportional to the longitudinal structure function F_{L}^{γ} can be neglected and the differential cross-section is directly proportional to F_2^{γ}, which is related to the sum over the quark parton distribution functions q^{γ} of the quasi-real photon, γ, via

$$F_2^{\gamma}(x,Q^2) = x\sum_{q=u,d,s}^{c,b,t} \mathrm{e}_{\mathrm{q}}^2\left[q^{\gamma}(x,Q^2) + \bar{q}^{\gamma}(x,Q^2)\right]. \qquad (2)$$

[1] Invited talk given at the PHOTON 2000 Conference, Ambleside, UK, August 26-31, 2000, to appear in the Proceedings.

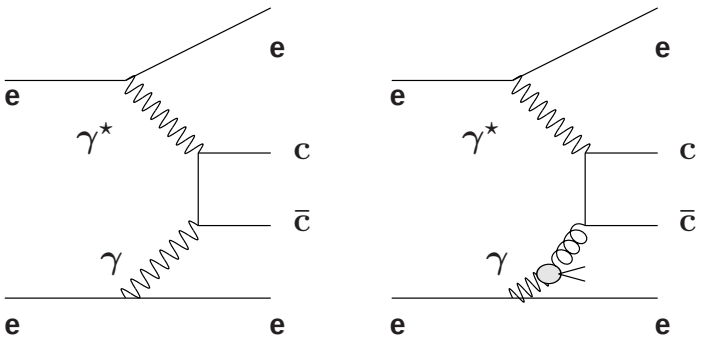

FIGURE 1. Examples of leading order diagrams contributing to (left) the point-like, and (right) the hadron-like part of $F_{2,\mathrm{c}}^{\gamma}$.

Due to the large scale established by their masses, the contribution to F_2^{γ} from heavy quarks can be calculated in perturbative QCD. At present collider energies only the contribution of charm quarks $F_{2,\mathrm{c}}^{\gamma}$ is important. Like the structure function for light quarks, $F_{2,\mathrm{c}}^{\gamma}$ receives contributions from the point-like and the hadron-like component of the photon shown in Figure 1.

Because of the charge of the charm quarks their contribution to F_2^{γ} is large and the importance increases for increasing values of Q^2, as can be seen from Figure 2, which shows the contributions from light quarks and from charm quarks separately, as predicted by the GRV parametrisations [3]. Charm quarks can only

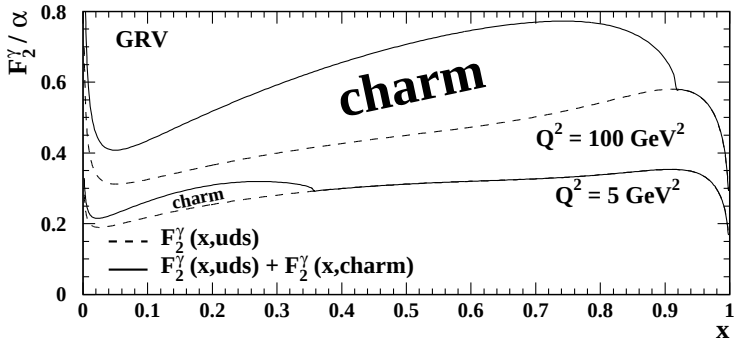

FIGURE 2. The structure function F_2^{γ} for u, d, s quarks alone and for u, d, s, c quarks, as a function of x and for two different values of Q^2.

be produced if the photon-photon invariant mass W is at least twice the mass of the charm quarks m_{c}. Using $x = Q^2/(Q^2 + W^2)$ this leads to the varying production threshold in x as a function of Q^2 seen in Figure 2.

Close to the production threshold, the point-like contribution to $F_{2,\mathrm{c}}^{\gamma}$ is accurately approximated by the prediction of the lowest order Bethe-Heitler formula. For quasi-real photons also the next-to-leading order (NLO) predictions have been calculated in [4]. For the hadron-like contribution the photon-quark coupling must be replaced by the gluon-quark coupling, and the Bethe-Heitler formula has to be integrated over the allowed range in fractional momentum of the gluon using a

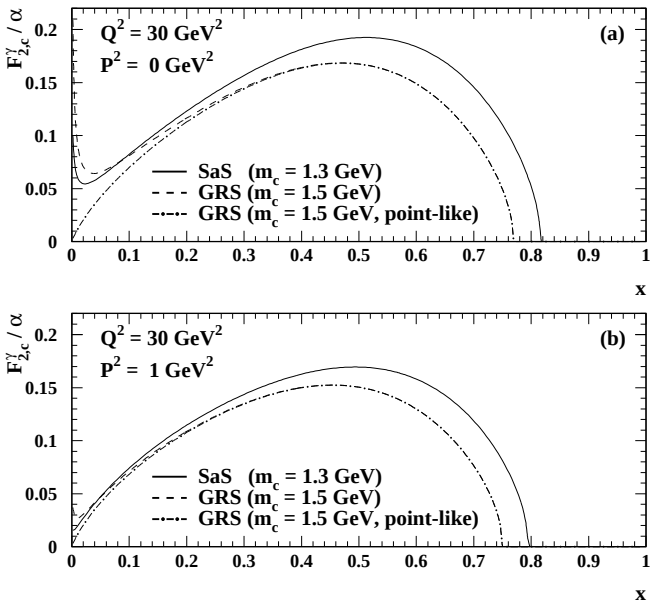

FIGURE 3. The predictions of the SaS1D (full) and the GRS (dash) parametrisations for $Q^2 = 30$ GeV^2 and for (a) $P^2 = 0$ and (b) $P^2 = 1$ GeV^2. In addition, the point-like contribution for $m_c = 1.5$ GeV(dot-dash) is shown.

parametrisation of the gluon distribution function of the photon, see e.g. [1].

The predicted behaviour of the point-like and hadron-like component of $F^{\gamma}_{2,c}$ for different values of m_c is shown in Figure 3, using the SaS1D [5] and GRS [6] parametrisations. For $x > 0.1$ the structure function is saturated by the point-like component which is only slowly suppressed for increasing virtualities P^2 of the quasi-real photon. In contrast, the hadron-like contribution dominates at small values of x and decreases much faster for increasing P^2. Finally, lowering the mass of the charm quarks leads to a higher threshold in x.

Given this predicted behaviour, the region of $x > 0.1$ can be used to test a purely perturbative NLO QCD prediction with only m_c and α_s as free parameters, and the low x behaviour mainly probes the gluon distribution function of the photon.

MONTE CARLO MODELS

The LO Monte Carlo generators HERWIG 5.9 [7] and Vermaseren [8] are used, both with $m_c = 1.5$ GeV. In HERWIG charm production is modelled using matrix elements for massless charm quarks, together with the GRV parametrisation for the parton distributions of the photon, again for massless charm quarks. The effect of the charm quark mass is only accounted for by not simulating events with $W < 2m_c$. Due to the massless approach used in HERWIG and the crude treatment at threshold, the predicted charm production cross-section is likely to be too large. The Vermaseren generator is based on the Quark Parton Model (QPM)

and consequently does not take into account the hadron-like component of the photon structure. However, the complete dependence of the cross-section on the different photon helicities is modelled.

THE MEASUREMENT OF $F_{2,c}^{\gamma}$

The measurement of $F_{2,c}^{\gamma}$ proceeds along the same lines as the measurement of F_2^{γ} with the addition of the identification of the charm quarks via the reconstruction of $D^{\star}$ mesons.

Events are selected with an energy of the scattered electron above 50 GeV, measured in the angular ranges (a) $33-55$ mrad or (b) $60-120$ mrad from either beam direction, thereby covering the approximate range in Q^2 of $5-100$ GeV^2. The visible hadronic mass $W_{\rm vis}$ is required to be below 60 GeV. Charm quarks are identified via $D^{\star} \to D^0\pi$, followed by $D^0 \to K\pi$ or $D^0 \to K\pi\pi\pi$. Using $f(c \to D^{\star}) = 0.235 \pm 0.011$ and the branching ratios of the D^0 decay modes of 0.02630 ± 0.00082 and 0.0519 ± 0.0029, this analysis covers only about 4% of all events containing a pair of charm quarks. For a clear acceptance the $D^{\star}$ mesons are further required to fulfill, $|\eta^{D^{\star}}| < 1.5$ and $p_T^{D^{\star}} > 1$ or 3 GeV for (a) or (b). Together with a typical selection efficiency of about 25% only about 1% of all $c\bar{c}$ events are positively identified.

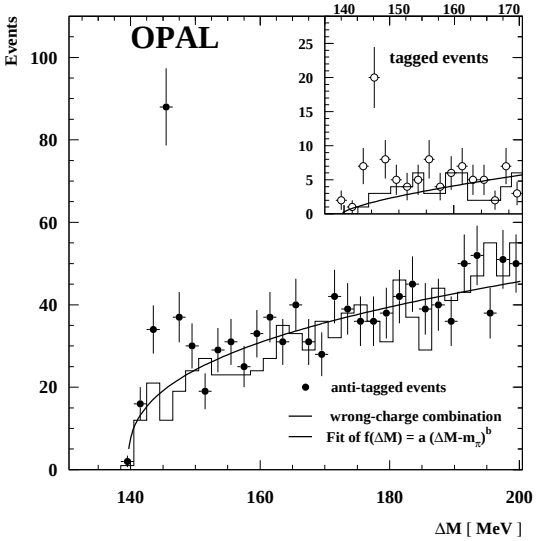

FIGURE 4. Mass difference ΔM for the anti-tagged and tagged sample.

Figure 4 shows the distribution of the difference between the $D^{\star}$ and the D^0 candidate mass. In both samples a clear peak is visible around $\Delta M = 145.4$ MeV. Subtracting the background, obtained from a fit to the upper sideband of the signal, 29.8 ± 5.9(stat) $D^{\star}$ mesons are found in the peak region.

Figure 5 shows the distributions of $W_{\rm vis}$ and of the measured Q^2 in comparison to the predictions of the HERWIG and Vermaseren Monte Carlo generators normalised

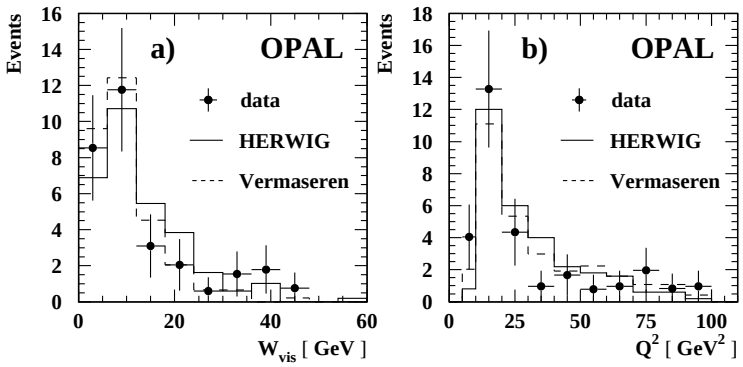

FIGURE 5. The distributions of a) the visible invariant mass $W_{\rm vis}$, and b) the negative four-momentum squared Q^2.

to the number of data events. Both Monte Carlo generators give a good description of the shape of the data distributions.

The cross-section for $\mathrm{D}^\star$ production is determined in the well-measured kinematic range described above. Based on this and the extrapolation factors obtained from the Monte Carlo models the full cross-section $\sigma(\mathrm{e^+e^-} \to \mathrm{e^+e^-c\bar{c}})$ and $F_{2,\mathrm{c}}^{\gamma}$ are evaluated in two bins of x with $0.0014 < x < 0.1$ and $0.1 < x < 0.87$.

For $x > 0.1$ the predictions of the Vermaseren and HERWIG Monte Carlo models are very similar. In contrast, for $x < 0.1$, there are two main differences. Firstly the selection efficiency for events with $\mathrm{D}^\star$ mesons fulfilling the kinematical requirements is different, and secondly, and even more important, the predicted cross-section within the invisible phase-space is largely different for the two models, resulting in different extrapolation factors, 12.9/5.1 for HERWIG/Vermaseren.

Since the hadron-like contribution is neglected in the QPM, the Vermaseren cross-section is much smaller than the LO and the NLO cross-section for $x < 0.1$. In contrast, mainly due to the massless approach taken, the prediction from HERWIG is higher than the cross-section from the LO and the NLO calculation. Therefore it is likely that the correct cross-section, and therefore the correct extrapolation factor, lies within the range of the two Monte Carlo predictions.

The measured $F_{2,\mathrm{c}}^{\gamma}$ for $\langle Q^2 \rangle = 20$ GeV^2 is shown in Figure 6. The central values are obtained by averaging the results using the HERWIG and Vermaseren Monte Carlo models, and half the difference is taken as extrapolation error, which dominates the uncertainty for $x < 0.1$. The NLO prediction is based on $m_{\mathrm{c}} = 1.5$ GeV, the renormalisation and factorisation scales are chosen to be $\mu_{\mathrm{R}} = \mu_{\mathrm{F}} = Q$, and the hadron-like contribution to $F_{2,\mathrm{c}}^{\gamma}$ uses the GRV parametrisation. The NLO corrections are small for the whole x range. The band for the NLO calculation is evaluated by varying m_{c} between 1.3 and 1.7 GeV and using $Q/2 \leq \mu_{\mathrm{R}} = \mu_{\mathrm{F}} \leq 2\ Q$.

For $x > 0.1$ the error of the measured cross-section is dominated by the statistical uncertainty, and the NLO calculation with only m_{c} and α_s as free parameters is in good agreement with the data. In contrast, for $x < 0.1$, the result suffers from the strong model dependence discussed above. Despite this uncertainty the corrected

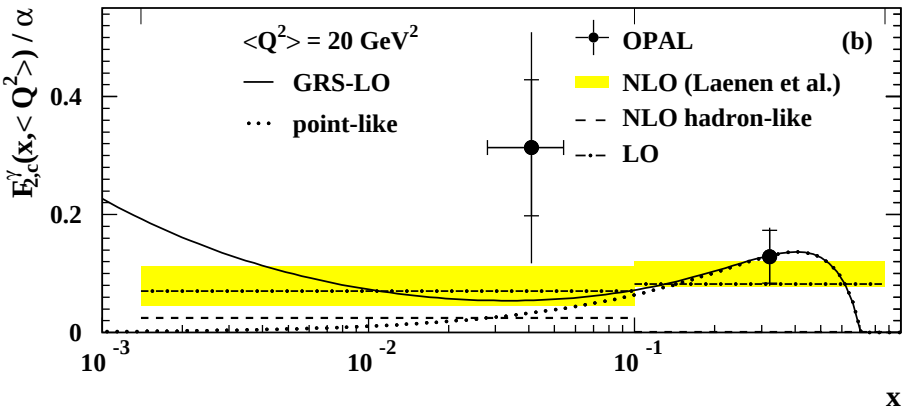

FIGURE 6. $F_{2,c}^{\gamma}$ compared to several predictions explained in the text.

data suggest a cross-section which is above the purely point-like component, i.e. the hadron-like component of $F_{2,c}^{\gamma}$ is non-zero.

Conclusion and Outlook

In conclusion, for $x > 0.1$, the purely perturbative NLO calculation is in good agreement with the measurement and for $x < 0.1$, the measurement suggests a non-zero hadron-like component of $F_{2,c}^{\gamma}$.

By using the massive matrix elements available in HERWIG6.1 and the full integrated luminosity of more than 500 pb^{-1} of the LEP2 programme, the measurement is likely to be improved considerably, both concerning the statistical and the systematic error.

Acknowledgement:
I wish to thank the organisers of this interesting conference, and especially Alex Finch. They created a fruitful atmosphere throughout the meeting and made attending the meeting a very nice experience.

REFERENCES

1. R. Nisius, Phys. Rep. **332**, 165 (2000).
2. OPAL Collab., G. Abbiendi et al., CERN-EP/99-157, accepted by Eur. Phys. J. **C**.
3. M. Glück, E. Reya, and A. Vogt, Phys. Rev. **D45**, 3986 and **D46**, 1973 (1992).
4. E. Laenen et al., Phys. Rev. **D49**, 5753 (1994).
5. G.A. Schuler and T. Sjöstrand, Z. Phys. **C68**, 607 (1995).
6. M. Glück, E. Reya, and M. Stratmann, Phys. Rev. **D51**, 3220 (1995).
7. G. Marchesini et al., Comp. Phys. Comm. **67**, 465 (1992).
8. R. Bhattacharya, G. Grammer Jr., and J. Smith, Phys. Rev. **D15**, 3267 (1977); J. Smith, J.A.M. Vermaseren, and G. Grammer Jr., Phys. Rev. **D15**, 3280 (1977).